

Finding the compositional diversity of the Solar System

J. de León¹, J. Licandro², M. Serra-Ricart², N. Pinilla-Alonso³, and H. Campins⁴

¹ Instituto de Astrofísica de Andalucía (CSIC), Glorieta de la Astronomía s/n, 18008 Granada, Spain

² Instituto de Astrofísica de Canarias (IAC), C/Vía Láctea s/n, 38205 La Laguna, Spain

³ NASA Ames Research Center, MS 245-3, Moffett Field, CA 94035-1000, USA

⁴ University of Central Florida, PO Box 162385, Orlando, FL 32816.2385, USA

Abstract

Asteroids can be defined as objects that do not have an atmosphere, are smaller than the planets and orbit the Sun. But, what is most important, asteroids are the remnants of the first forming blocks of the Solar System. The main asteroid population is located between the orbits of Mars and Jupiter, in a region called the Main Belt (MB). Other important populations are near-Earth asteroids (NEAs) and Mars crossers (MCs). In the outer Solar System, cold, icy bodies that are located beyond the orbit of Neptune are called trans-neptunian objects (TNOs), and concentrate in a region known as the Kuiper Belt. Visible and near-infrared reflectance spectra of all these “minor bodies”, obtained from ground-based observations, are modelled using different techniques, and, together with laboratory experiments with analogue materials (both terrestrial and from meteorites), they allow us to infer information about several properties, like surface composition, particle size distribution or the effects of space weathering. The analysis of the physical and dynamical properties of these objects, as well as their surface composition is of particular interest, as it is fundamental to understand the processes involved in the formation and subsequent evolution of the Solar System.

1 Introduction

The general view of our Solar System has slightly changed during the last decades. After the General Assembly of the International Astronomical Union, held in Prague in the summer of 2006, bodies (except satellites) in our Solar System can be separated into three main categories: planets (have enough mass to be in hydrostatic equilibrium and to clear the neighbourhood of their orbits), dwarf planets (the same as planets, but have not cleared

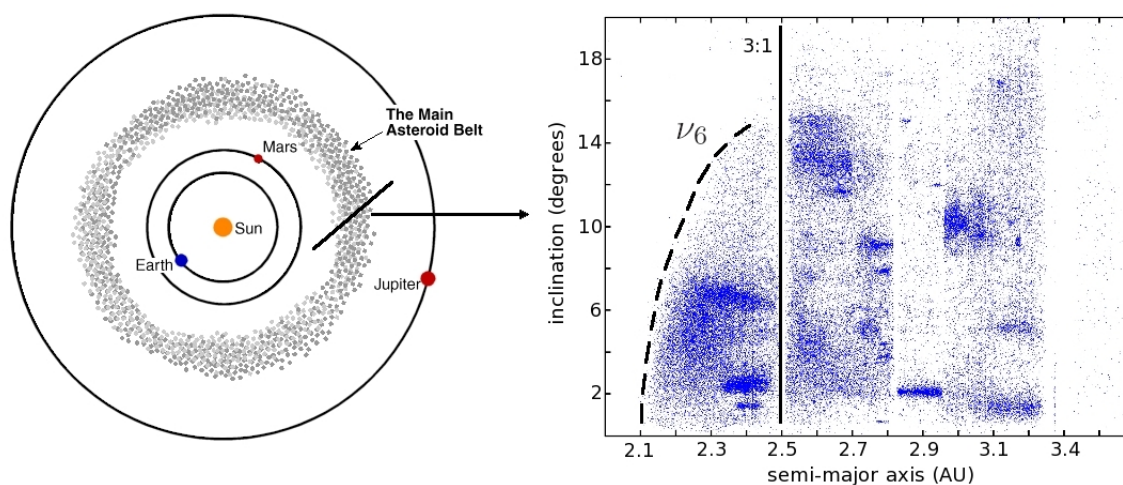


Figure 1: Schematic view (from top) of the inner planets and the main asteroid belt. The distribution of the asteroids in the belt is not uniform, and there are gaps and clumps created by the gravitational resonances mainly due to Jupiter and Saturn. The 3:1 mean-motion resonance with Jupiter (at 2.5 AU) and the ν_6 secular resonance with Saturn are the two main transport routes to deliver asteroids from the main belt to the near-Earth space.

their neighbourhood), and the rest of objects (not satellites), referred as small (or “minor”) Solar System bodies, including asteroids and comets.

Our Solar System can be roughly divided into two parts, being the orbit of Jupiter the usual divisory line. In the inner Solar System (up to Jupiter), the main concentration of minor bodies is located between Mars and Jupiter (1.52–5.20 AU), and is called the Main Belt (MB). The distribution of objects in the main asteroid belt is not uniform. The presence of the planets, in particular Jupiter, produces gravitational resonances (mean-motion or secular) that create “gaps” and clusters of objects, modelling the shape of the belt (see Fig. 1). Collisional events also generate groups or “families” of objects that share similar orbital characteristics. Besides the MB population, and apart from the asteroids whose orbits cross the orbit of Mars and have perihelion distances between 1.30 and 1.66 AU (Mars crossers), the other big population of objects is located in the near-Earth space (their orbits are confined between the Earth and Mars perihelions), and is composed of both asteroids and comets. The dynamical life-times of near-Earth objects (NEOs) are short compared to the age of the Solar System, and so this population must be periodically replenished. Besides some uncertain fraction that comes from dead or dormant comets, near-Earth asteroids come primarily from the Main Belt. [7] showed that the two main transport routes for asteroids to reach the near-Earth space are the 3:1 mean-motion resonance, located at 2.5 AU, and the ν_6 secular resonance, in the inner part of the belt (Fig. 1). Finally, there are also objects orbiting in the Lagrangian points of the orbits of a planet, called Trojans, like Jupiter (the most numerous) and Mars Trojans.

Apart from the Centaurs, that share characteristics of both asteroids and comets and

are located between the orbit of Jupiter and Neptune, the main population of objects in the outer Solar System are the trans-Neptunian objects (TNOs). By definition, a TNO is any minor body that orbits the Sun at a greater distance on average than Neptune. This huge volume space is usually divided into the Kuiper Belt, the scattered disk and the Oort cloud. The Kuiper belt is a dynamically stable region similar to the asteroid main belt, that extends from 30 to 55 AU approximately and is about 20 to 200 times as massive. The scattered disk is composed of objects that have extreme orbits, believed to be the result of gravitational scattering by the giant planets (their orbits can extend well beyond 100 AU). This region is considered to be the origin for most periodic comets. The Oort cloud, an hypothesized spherical cloud of objects at 50000 AU from the Sun, is believed to be the source of most long-period and Halley-type comets, and also a reservoir of trans-Neptunian objects. Since the discovery of Pluto's moon, Charon, in 1978, over 1000 TNOs have been discovered, with different sizes and composition. Eris is the largest known TNO, and its discovery led to the definition of dwarf planets mentioned above.

2 Compositional context

Minor bodies present a wide variety of compositions, and so the diversity of materials that can be found when we study their surfaces is remarkable. Objects located in the outer part of the Solar System are cold enough to be composed mainly of ices of different materials, like water, methane or ammonia. While we get closer to the Sun and temperatures increase, the most abundant materials are silicates (olivine, pyroxene, feldspar), and we find also metals (Fe,Ni), and carbon compounds. The presence of water is also significant at these distances, usually in the form of aqueous altered minerals, like phyllosilicates.

2.1 Icy bodies: TNOs and comets

TNOs are thought to be low density mixtures of rock and ice, with some organic material. Composition is usually inferred from reflectance spectra of the surface of the objects. They present a wide range of spectra, differing in reflectivity in visible and near infrared (see Fig. 2). Neutral objects present a flat spectrum, reflecting as much infrared as visible spectrum [2]. Very red objects present a steep slope, reflecting much more in the infrared. Typical models of the surface include water ice, amorphous carbon, silicates and organic macromolecules, named "tholins"¹, created by intense radiation.

Kuiper belt objects (KBOs) are primarily composed of ices, a mixture of light hydrocarbons (such as methane), ammonia, and water ice. At the location of the Kuiper belt, the temperature is only about 50K, so many compounds that would be gaseous closer to the Sun remain solid [35]. Observations of small Kuiper Belt objects find that these bodies have mostly dark neutral to reddish spectra with faint or no features. These surfaces are thought to be covered by a mixture of silicates, carbon and in some cases small amounts of water-ice

¹Tholins: term used first by [47] to refer to synthetic complex organic solids, showing colours ranging from yellow through red to black, and formed by irradiation of ices containing simple hydrocarbons and nitrogen

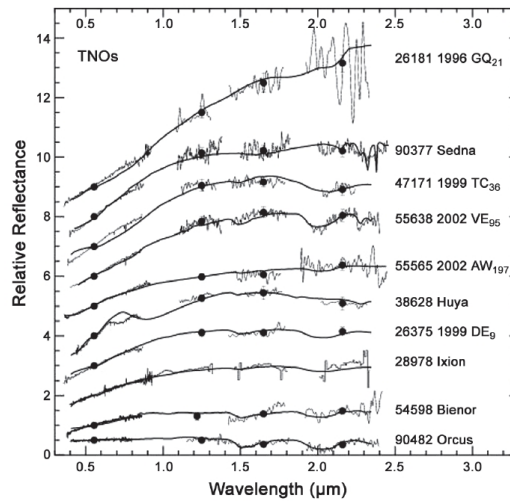


Figure 2: Visible and near-infrared spectra of some TNOs. The points correspond to broadband photometric measurements at $V, J, H,$ and K . The continuous lines superimposed on the spectra are the best-fit spectral models. Absorption bands due to the presence of water (at 1.5 and 2.0 μm) and methane (at 2.4 μm) are present in almost all the spectra. Figure taken and modified from [3].

[43, 39, 29]. Some other TNOs and Centaurs [19, 24] exhibit red slopes in the visible that have been modelled with tholins as the principal refractory component, giving the overall colour over the wavelength 0.5-2.5 μm . The recent discoveries of volatiles (methane and nitrogen) on large KBOs Eris, Makemake and Sedna have shown that these objects are part of a new class of volatile-rich bodies in the outer Solar System [40, 41, 24].

2.2 Asteroids

The inner Solar System is mainly populated with asteroids. Asteroids located in the main belt, near-Earth asteroids and Mars Crossers can be divided into two big groups, well differentiated in terms of mineralogical composition: rocky or “stony” objects (S), composed of silicates and metal, and carbonaceous objects (C), composed of carbon and opaque materials (see Fig. 3). The main asteroid belt is the principal source for near-Earth asteroids and Mars crossers. Main motion and secular resonances with Jupiter and Saturn have an enormous influence on the eccentricity and the inclination of the objects that get too close to them, changing their orbits and sending them to the near-Earth space. Therefore, the materials and compositions that are found in the main belt are well representative of the other two populations.

Within the main two taxonomical groups, there are further sub-classes according to the relative proportions of different minerals that are present on the surface of the objects. Among the rocky asteroids, or S-class asteroids, we can find asteroids composed mainly of

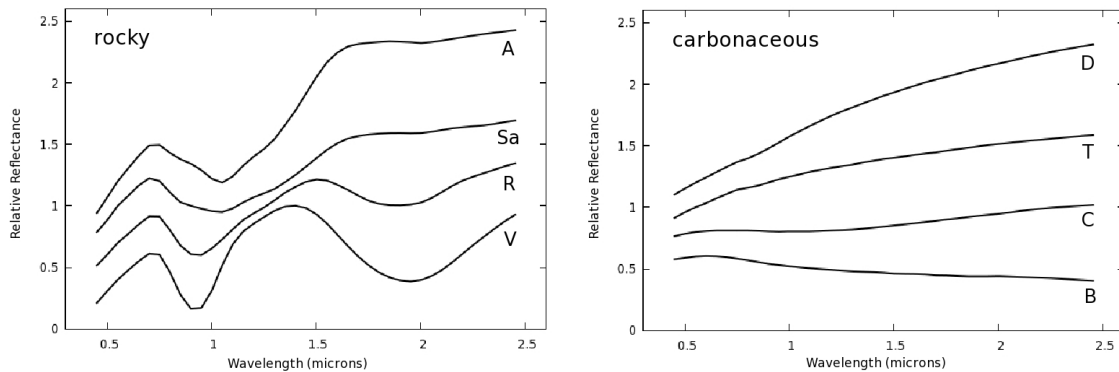


Figure 3: Visible and near-infrared reflectance spectra of some of the taxonomic classes that can be found in the asteroid belt. Rocky asteroids present characteristic absorption features due to the presence of silicates, while carbonaceous asteroids usually have featureless spectra, with spectral slopes ranging from blue (B-type) to red (D-type).

olivine (A-type asteroids) or asteroids composed of mixtures of pyroxene and feldspar (V-type asteroids, after the differentiated asteroid (4) Vesta). S-type asteroids are composed of mixtures of olivine, pyroxenes, plagioclase and metals.

The two main taxonomical classes of asteroids, rocky and carbonaceous, are distributed in opposite ways in the main asteroid belt: while S-type objects concentrate in the inner part, carbonaceous, C-type asteroids are more abundant in the outer part of the main belt. As the two main source of near-Earth asteroids are the gravitational resonances located in the inner part of the belt, it is expected (and in fact confirmed by observational surveys) that the majority of NEAs belong to the S-class, that is to say, are composed of silicates.

3 Meteorites

A meteorite is defined as “a natural object that survives its fall to Earth from space” [34]. As it orbits the Sun, the Earth constantly encounters solid objects, or meteoroids, of varying sizes. Larger and faster objects survive the heating produced by friction when entering the atmosphere, and can be recovered for their analysis. The general composition, mineralogy and petrology of a meteorite is related to that of its parent body, and to the amount of processing it has suffered. In fact, we can say that meteorites spend part of their life-times as near-Earth asteroids, and in this sense, their study is crucial to understand this population.

Meteorites are assigned to three categories on the basis of their contents of metallic iron-nickel (Fe-Ni) and silicates. *Stony* meteorites consist principally of silicates, *stony irons* contain roughly equal proportions of metal and silicates, and *iron* meteorites consist almost wholly of metal. Stony meteorites are subdivided into two main groups, depending on the presence (*chondrites*) or not (*achondrites*) of chondrules, generally mm-sized, near spherical masses of primordial silicates. These spheres have not melted since they formed by the accretion of their different constituents. Chondrites have chemical compositions that closely

resemble that of the volatile-free Sun (they are chemically primitive), and in this sense they provide valuable information about the early Solar System. We can distinguish between *carbonaceous chondrites* (CC), formed in oxygen rich regions of the early Solar System, so that most of their metal appears in form of silicates, oxides and sulfides; and *ordinary chondrites*, the most abundant, accounting for more than 80% of the falls. Ordinary chondrites (OCs) are divided into three subgroups, according to their decreasing Fe content and their increasing olivine content: H, L and LL chondrites. H chondrites present a $\sim 18\%$ volume in metal content, and their olivine/pyroxene ratio is about 56/46, while LL chondrites barely reach a $\sim 4\%$ in metal content and present the highest olivine/pyroxene ratio, about 66/34 [12].

Differentiated meteorites or *achondrites* present a remarkable diversity, from partially melted and recrystallized achondrites (the rarest), to igneous rocks, more abundant, or mechanical mixtures of igneous fragments derived from them (*breccias*²). Primitive achondrites have suffered from partial melting and differentiation in their chondritic parent body, and in this way they have a similar composition to the most primordial chondrites. Among primitive achondrites we find several groups, each one with its own characteristics (Acapulcoites, Lodranites, Brachinites, etc.). The rest of the achondrites are divided into four main groups: the HED group (Howardites-Eucrites-Diogenites), associated with asteroid (4) Vesta, the SNC group (Shergottites-Nakhlites-Chassignites), associated with Mars [56], the group associated with the Moon and other evolved achondrites, like angrites and aubrites.

3.1 Ordinary chondrites and S-type asteroids

Ordinary chondrites are composed of abundant chondrules containing olivine, pyroxene and plagioclase feldspar, with lesser amounts of an olivine-rich matrix, metals and sulfides [9]. Spectrally, ordinary chondrites have features due to olivine and pyroxene (see Fig. 3) that are seen also in the spectra of S-type asteroids. These are the most abundant type of asteroids observed in the inner belt, and they are also the most abundant within the NEA population. Therefore, S-type asteroids have long been considered the most likely parent bodies of the ordinary chondrites. However, they are spectrally redder than OCs and tend to have weaker absorption bands. This reddening and “darkening” is caused by the space weathering, i.e., any surface modification process that changes optical properties, physical structure or chemical or mineralogical properties of an airless body. Space weathering [44, 10] is believed to be induced by two main processes: irradiation by cosmic and solar wind ions, and bombardment by interplanetary dust particles (micro-meteorites).

On the other hand, the best spectral matches to ordinary chondrites are in the near-Earth population [5]. There seems to be a continuum of spectral properties between the S asteroids and the OCs among the Q- and S-type NEAs in the visible and near-infrared (see Fig. 4). This may be related to surface gravity and/or surface age, because the NEAs are much smaller and should have much younger surfaces (on average) than main-belt objects [6].

²The word *breccias* comes from Latin and it means literally “broken stone”. There are different types of breccia, depending on the process that generates the mixture of the material.

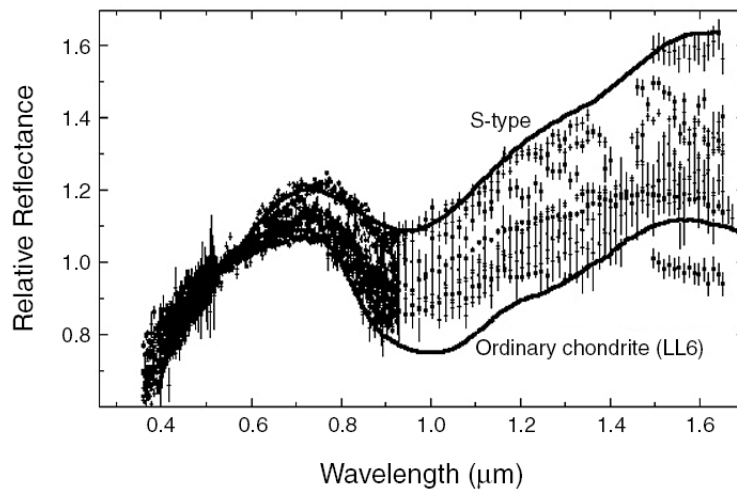


Figure 4: S-type asteroids present on average redder surfaces than ordinary chondrites (two continuous lines). The data displayed between these two curves correspond to Q- and S-type NEAs, showing an apparently continuous distribution of spectral properties between S-type asteroids and OCs. Figure taken from [5].

3.2 HED meteorites and V-type asteroids

The HED group (also called basaltic achondrites) is the most abundant group of achondrites and have suffered from igneous differentiation processes similar to those observed on the Earth's magmatic rocks, like basalts. Crystallization ages inferred from isotopic abundances, between 4.4 and 4.5 Gyr, show that HED meteorites come from one single parent body, relatively large (few hundred kilometres), with a short but intense igneous history. [18] first pointed at asteroid (4) Vesta as the most likely parent body of HED meteorites, because it is the only large body surviving with an impact “basaltic” crust. Smaller V-type asteroids have been found in the Vesta family, called “vestoids” [4, 23]. However, the number of grouped and ungrouped iron meteorites imply the formation and later disruption of at least 50 differentiated parent bodies [8]. Recent observational and meteoritical evidences support the existence of at least two more “Vestas”: asteroid (1459) Magnya [38] and asteroid (21238) 1995 WV7 [30].

3.3 Carbonaceous chondrites and C-type asteroids

Carbonaceous chondrites and, in particular, CM chondrites have been generally linked to C-type asteroids. CM chondrites have low visible albedo (~ 0.04), relatively strong UV features, weak features between 0.6 and 0.9 μm and featureless spectra from 0.9 to 2.5 μm [36, 55]. The strongest of those weak features located between 0.6 and 0.9 μm is an absorption band centred at 0.7 μm , attributed to ferric iron (Fe^{3+}) in the phyllosilicates. CM chondrites are typically composed of small chondrules set in an aqueously altered matrix of Fe^{3+} -bearing

phyllosilicates (6-12 % of water). C-type asteroids also have low albedos and relatively featureless spectra and almost half of the C-type asteroids in the main belt present the 0.7 μm absorption feature associated with water.

4 Methods to extract compositional information

Mineralogical characterization of the material on the surface of an asteroid relies primarily on the interpretation of the observable diagnostic properties to determine the presence, abundance and/or composition of one or more mineral or chemical species. Those mineral species are analysed in the laboratory, by means of transmission and reflection spectra, simulating different incidence and view angles, varying temperature, grain size, weight percentage of mineral phases in mixtures, etc. All these calibrations help us to characterise the reflectance spectrum of the object we want to study.

Fortunately, a number of the most abundant and important minerals do exhibit diagnostic features in the visible and near-infrared wavelength region. The most important set are crystal field absorptions [13] arising from the presence of transition metal ions (most commonly Fe^{2+}) located in specific crystallographic sites in mafic (Mg- and Fe-bearing) silicate minerals (olivine, pyroxene, etc). Olivine presents a wide and very characteristic absorption feature at 1 μm [37], as the result of the superposition of three individual absorption bands associated with the location of Fe^{2+} cations in particular crystallographic sites; plagioclase (feldspar) has an absorption band centred at 1.2 μm ; pyroxenes show two absorption bands at 1 and 2 μm , and the position of their centres changes as a function of the concentrations of Fe^{2+} and Ca^{2+} [1]. Aqueous altered minerals, such as phyllosilicates, show absorption bands centred around 0.7 μm , attributed to $\text{Fe}^{2+} \rightarrow \text{Fe}^{3+}$ charge transfer in iron oxides. In the case of more distant and cold objects, like TNOs, signatures of water ice are present at 1.5, 1.65, 2.0 μm , and signatures of other ices include those due to CH_4 around 1.7 and 2.3, CH_3OH at 2.27 μm , and NH_3 at 2 and 2.25 μm , as well as solid C-N bearing material at 2.2 μm [3].

4.1 Taxonomy

There exist a number of methods to interpret mineralogy of an asteroid from its reflectance spectrum. The first and most evident is to establish a taxonomy in terms of differences in the spectra and to assign each taxonomic type to a particular composition. In the case of asteroids, taxonomies have been historically developed from visible spectra, accounting for variations in spectral slope, albedo and presence of particular absorption features [53, 14]. Recently, an extension of these taxonomies to the near-infrared (up to 2.5 μm) has been developed [22], although the main taxonomic types have not significantly changed.

4.2 Laboratory spectral studies

The calibrations needed in order to properly interpret the mineralogy of an asteroid are largely derived from laboratory spectral studies of meteorites and mineral mixtures intended

to simulate asteroid lithologies. Meteorites are analysed in the laboratory to obtain petrological and mineralogical information, as well as bulk-chemical and isotopic properties in order to separate them into groups. Important parameters for silicate-bearing meteorites include abundance of refractory elements (Ca, Al, Ti), FeO concentrations in olivine and orthopyroxene, and whole-rock oxygen-isotopic composition. Phase separation by physical means followed by selective chemical attack has been the established, or “classical” method of meteorite analysis. It provides reliable measurements of total Fe, SiO₂ and MgO contents, information on the distribution of Fe between metal, sulfides and oxidized phases, and the determination of water and carbon contents. Other instrumental and less destructive methods of chemical analysis include X-ray fluorescence (XRF), neutron activation analysis (NAA), Raman spectroscopy, etc. Among others, some typical analysis are the determination of concentrations of rare Earth elements (REE), the comparison of relative abundances of radioisotopes and daughter pairs to compute CRE ages [25], the oxygen isotopic measurements that are used to distinguish between different meteorite groups, and the transmission/scanning electron microscopy (TEM/SEM) images and back-scattered electron images (BSE) of thin sections to study the meteorite to the smallest scales (inclusions, nodules, inter-granular veins, grain rims, etc) and to determine their petrologic types.

Laboratory experiments include also the characterization of different materials that can be found on the surface of the objects we study. Reflectance spectra in the visible and near-infrared of most common silicates (olivine, pyroxene) are obtained in the laboratory, as well as intimate mixtures of several mineral components (silicates, sulfides, metals), varying their relative weight proportion, grain sizes, modal phases, etc. Systematic variations in their reflectance spectra are used as constraints when interpreting the spectra of our target bodies. Finally, the experimental approach is also employed to simulate the effects of the space weathering: samples of meteorites, silicates and ices are irradiated with highly charged ions (solar wind particles) and laser nano-phase pulses (micrometeorite bombardment).

4.3 Curve matching

For many years, analysis of asteroid reflectance spectra relied on a comparison to laboratory reflectance spectra of meteorites. This technique provides important insights into plausible surface mineralogies, although it presents some limitations: a lack of enough meteorite analogues; spectral variations associated with changes in grain size, temperature, viewing geometry; the effects such as space weathering. Nevertheless, curve matching is still useful as an initial input for a more detailed mineralogical analysis.

4.4 Spectral parametrization

Crystal field absorption bands associated with mafic minerals (olivine, pyroxene, plagioclase, etc.) appear in the majority of reflectance spectra of the asteroids. Therefore, the mineralogy of an asteroid can be characterised by the parametrization of its reflectance spectrum. The wavelength position, width, and intensity of those crystal-field absorption bands are controlled by structure and composition that are directly related to the fundamental definition of the

mineral.

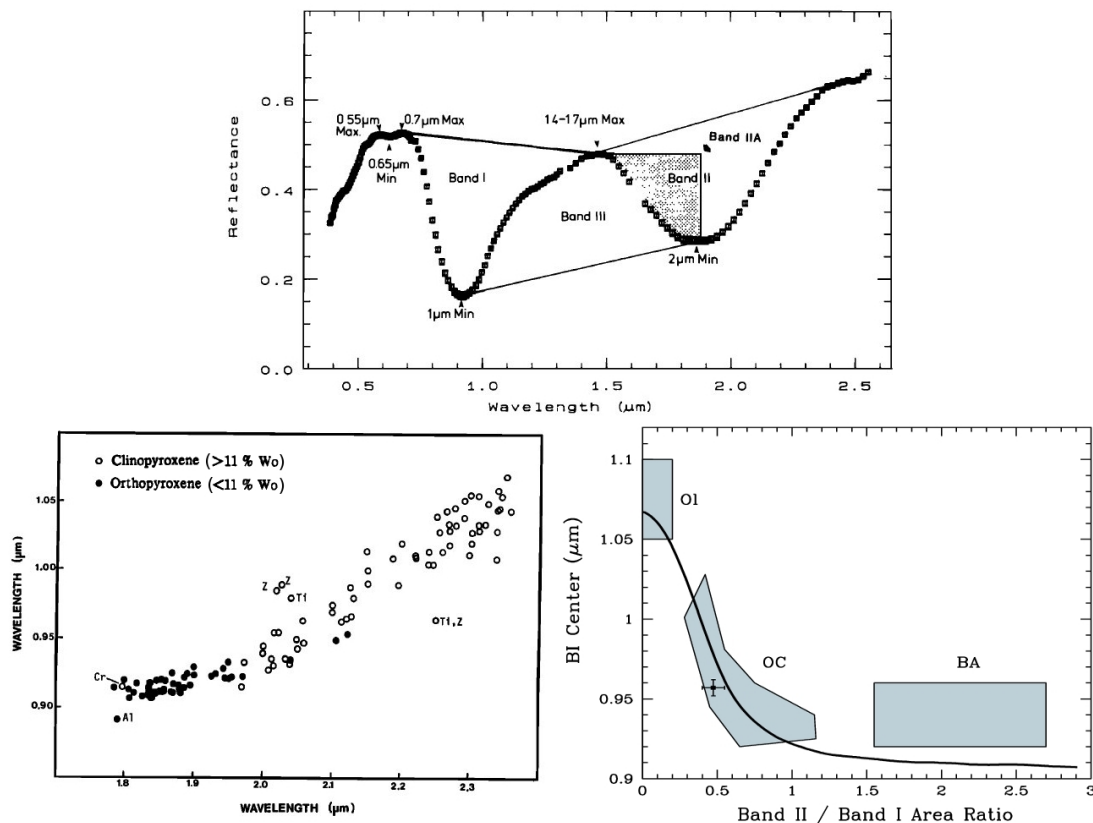


Figure 5: From top to bottom, counter-clockwise: spectrum of a mixture of olivine and pyroxene, showing some of the spectral features selected as diagnostic, as the band centres or the band areas [17]; wavelengths of centres of absorption bands near 1 and 2 μm in the reflectance spectra of pyroxenes. Orthopyroxene (low-Ca pyroxene, < 11 % Wo) bands shift to longer wavelengths with increasing Fe content, whereas clinopyroxene (high-Ca pyroxene, > 11 % Wo) bands do it with increasing Ca content [16]; centre of the absorption band around 1 μm versus the band area ratio (BAR). The three coloured regions are defined by meteorite spectra by [28], and corresponds to monomineralic olivine assemblages (OI), ordinary chondrites (OC) and basaltic achondrites (BA). The solid line indicates the olivine-orthopyroxene mixing line (figure taken from [26]).

The relationship between diagnostic spectral parameters (absorption band centre positions, band area ratio, depth, etc) for reflectance spectra of a number of mafic minerals, in particular olivine and pyroxene, was first outlined by [1] and revisited by [17, 16] and [28]. The variation of each spectral parameter or combination of parameters provide different mineralogical information. For example, [1] measured the positions of the centres of the two absorption bands at 1 and 2 μm for a mixture of ortho and clinopyroxenes (see Fig. 5), finding that those positions are shifted systematically to longer wavelengths with increasing Fe

and Ca content respectively. [17] measured the band area ratio (BAR) of a controlled sample of more than 70 mixtures of olivine and orthopyroxene, using different weight proportions and grain sizes. They found that the relationship between the olivine/pyroxene ratio and the BAR parameter was linear within 10% and 90% of pyroxene abundance. [28] analysed the spectra of 40 S-type asteroids and compared the computed spectral parameters (centre of band *I*, near 1 μm , and band area ratio) with those obtained for a sample of meteorites (Fig. 5). With the computed values, they defined three distinct regions: one associated to monomineralic assemblages of olivine (Ol), another representing ordinary chondrites (OC) and a third one for basaltic achondrites (BA), dominated by pyroxenes. Depending on its position relative to these regions in this calibration plot, one could infer the mineralogy on the surface of an asteroid.

4.5 Models

Another way to infer the surface composition of an object from its reflectance spectrum is to use models to calculate a synthetic spectrum for comparison with the observational data. Two approaches are usually applied: the radiative transfer theory to describe light scattering from dispersed particulate media, and deconvolution of the spectrum into its individual absorption bands via mathematical functions.

The two most commonly used methods based on light scattering are those of [31] and [49]. The methods use the radiative transfer equation within a small elementary volume of the scattering medium, which is characterised by the albedo of single scattering. Hapke model computes the bidirectional reflectance of a medium composed of spheroidal, closely packed particles of a single component. The model can be applied also to intimate mixtures of different components, and is valid for grain sizes that are large compared to the wavelength. Several subsequent improvements take into account rough surfaces [32] and space weathering [33]. In the model by [49], multiple reflections in a particle are considered as multiple-scattering in a one-dimensional medium with the same effective reflection coefficients. As major differences with Hapke model are that Shkuratov takes into account the porosity of the medium and that observational geometry is not mentioned, contrary to that of Hapke. Fig. 6 shows one example of the use of each of these models to fit the reflectance spectra of one asteroid and one TNO.

Finally, another way of modelling the reflectance spectra of asteroids is to use a deconvolution method that accurately represents absorption bands as discrete mathematical distributions and resolves composite absorption features into individual absorption bands. This method was developed by [52] and called Modified Gaussian Model (MGM), as it uses gaussian distributions with altered symmetry (relative slope of the right and left wings) to describe the Fe^{2+} electronic transition absorption bands present in the majority of silicates (mainly olivine and pyroxene). The MGM accurately describes the shape of electronic transition absorptions that occur when photons interact with ions in distorted crystal field sites.

In this way, each individual modified gaussian is characterised by three free parameters: centre, width and strength (amplitude). The absorption bands are all superimposed onto a continuum, which is modelled as a straight line in energy, and represented by two additional

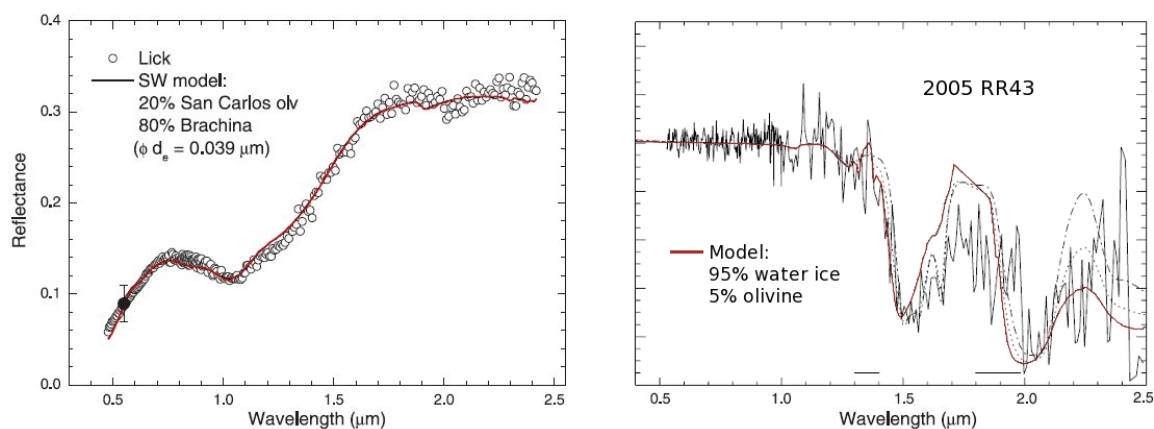


Figure 6: Two examples of the radiative transfer models by Hapke (left) and Shkuratov (right). The spectrum of near-Earth asteroid (1951) Lick have been best fit (red curve) with a linear combination of 20% of San Carlos olivine and 80% of Brachina meteorite, using a nano-phase iron model to account for the space weathering [11]. One of the possible fits (red curve) of the spectrum of TNO 2005 RR43 obtained with the Shkuratov approximation and an intimate mixture of 95% amorphous water ice and 5% olivine [45].

parameters. This means that, for the simplest case of olivine, which has one single absorption band centred around $1 \mu\text{m}$ formed by the superposition of three individual bands, we have a total of $3 \times 3 + 2 = 11$ free parameters. Therefore, it is mandatory to have some constraints to the model, otherwise one could fit any spectra just by adding enough number of individual gaussians. MGM analysis of laboratory spectra of silicates [50, 51] form a standard for comparison to remotely acquired spectra, and in this sense, before any fit can confidently be interpreted in terms of composition, it must conform to all the results of the laboratory studies.

One recent revision of this MGM method has been developed by [46] and called Exponential Gaussian Optimization (EGO). The general EGO equation has been especially designed to account for absorption bands affected by saturation and asymmetry.

5 Recent results

In the last few years, there have been some remarkable findings that might change the way we understand our current view of the Solar System in terms of composition:

- *Near-Earth asteroids are olivine rich.* As mentioned in Section 3.1, it has been generally and long assumed that near-Earth asteroids are the most likely parent bodies of the ordinary chondrites. The majority of NEAs are rocky asteroids, and they present the same absorption bands due to silicates that are present in the spectra of OCs, the most abundant class of meteorites. Recent mineralogical analysis of statistically significant

numbers of NEAs performed by different authors [54, 21, 27] show that NEAs present on average a high olivine content, similar to what is found for LL chondrites, a subgroup of ordinary chondrites. This is quite a puzzling result, as LL chondrites constitute only a 7% of the overall meteorite falls. A size distribution influence of the YORP effect that moves objects from the main belt into the resonances, or the over classification of L chondrites as LL chondrites, are two of the several explanations that have been invoked to explain this very new result.

- *Water in the Main Belt?* It has been commonly accepted that the two major reservoirs of comets are the Kuiper belt and the Oort Cloud. Those reservoirs are located beyond the orbit of Neptune, where temperatures are low enough for water to condense as ice. Nevertheless, water is stable as ice down to much smaller heliocentric distances, so it has long been suspected that other populations (like Hildas at 4AU or Trojans at 5AU) might be ice-rich, dormant comets. Recent discoveries of a population of comets originating in a third reservoir, the main asteroid belt, lends new support to the idea that main-belt objects could be a major source of terrestrial water. Although no measurements of water ice on asteroids had been made so far, its presence had been inferred from the activity of main-belt comets. Two recent publications by [15] and [42] show the first direct detection of water ice on the surface to two main belt asteroids: (24) Themis and (65) Cybele. Water ice and organic compounds are prevalent on the surface of Themis, something unexpected due to the relatively short lifetime of exposed ice at this distance (3.2 AU) from the Sun. Nevertheless, there are several plausible sources, such as a subsurface reservoir that brings water to the surface through “impact gardening” and/or sublimation. In the case of (65) Cybele, its surface is covered by a fine anhydrous silicate grains, with a small amount of water ice and complex organics. Main difference with asteroid (24) Themis is in the composition of the organics.
- *Origin of NEA (3200) Phaethon.* Asteroid (3200) Phaethon is a remarkable Near Earth asteroid. It was the first asteroid associated with a meteor shower (Geminid stream). Phaethon's unusual orbit has a high inclination and a very low perihelion distance (0.14 AU). Its reflectance spectrum suggests a connection with primitive meteorites, best fitting with CI/CM carbonaceous chondrites, aqueously altered and rich in hydrated silicates. However, its origin is not well determined. In a recent paper, [20] show that the most likely source of Phaethon and the Geminids is the asteroid (2) Pallas, one of the largest asteroids in the main belt, which is surrounded by a collisional family, containing several Phaethon-sized objects. Pallas highly inclined orbit and surface composition, also primitive and with evidence of hydration, support this connection. Their analysis reveals a striking similarity between Phaethon's visual spectrum and those of Pallas family members. Spectral comparison excludes also any other B-type asteroid in the main belt as a possible parent body of Phaethon. Numerical simulations show the existence of a robust dynamical pathway, connecting the orbital neighbourhood of Pallas with that of Phaethon. In this way, Pallas is the most likely parent body of Phaethon, and the Pallas family may constitute a potential source of primitive NEAs.

References

- [1] Adams, J. B. 1974, *J. Geophys. Res.*, 79, 32
- [2] Barucci, M. A., & Peixinho, N. 2006, *Proceedings of the IAU Symposium*, 229, 171
- [3] Barucci, M. A., Brown, M. E., Emery, J. P., et al. 2008, *The Solar System Beyond Neptune*, 143
- [4] Binzel, R. P., & Xu, S. 1993, *Science*, 260, 186
- [5] Binzel, R. P., Lupishko, D. F., Di Martino, M., et al. 2002, in *Asteroids III*, ed. W. F. Bottke Jr., A. Cellino, P. Paolicchi, & R. P. Binzel (Tucson: University of Arizona Press), 255
- [6] Binzel, R. P., Rivkin, A. S., Stuart, J. S., et al. 2004, *Icarus*, 170, 259
- [7] Bottke, W. F., Morbidelli, A., Jedicke, R., et al. 2002, *Icarus*, 156, 399
- [8] Bottke, W. F., Nesvorný, D., Grimm, R. E., et al. 2006, *Nature*, 439, L821
- [9] Brearley, A. J., & Jones, R. H. 1998, in *Reviews in Mineralogy*, Vol. 36: *Planetary Materials*, ed. J. J. Papike (Washington: Mineralogical Society of America), 1
- [10] Brunetto, R., & Strazzulla, G. 2005, *Icarus*, 179, 265
- [11] Brunetto, R., de León, J., & Licandro, J. 2007, *A&A*, 472, 653
- [12] Burbine, T. H., McCoy, T. J., Meibom, A., et al. 2002, in *Asteroids III*, ed. W. F. Bottke Jr., A. Cellino, P. Paolicchi, & R. P. Binzel (Tucson: University of Arizona Press), 653
- [13] Burns, R. G. 1970, *Mineralogical Applications of Crystal Field Theory* (Cambridge: Cambridge University Press)
- [14] Bus, S. J., & Binzel, R. P. 2002, *Icarus*, 158, 106
- [15] Campins, H., Hargrove, K., Pinilla-Alonso, N., et al. 2010, *Nature*, 464, L29
- [16] Cloutis, E. A., & Gaffey, M. J. 1991, *J. Geophys. Res.*, 96, 22809
- [17] Cloutis, E. A., Gaffey, M. J., Jackowski, T. L., et al. 1986, *J. Geophys. Res.*, 91, 11641
- [18] Consolmagno, G. J., & Drake, M. J. 1977, *Geochim. Cosmochim. Acta*, 41, 1271
- [19] Cruikshank, D. P., Roush, T. L., Bartholomew, M. J., et al. 1998, *Icarus*, 135, 389
- [20] de León, J., Campins, H., Tsiganis, K., et al. 2010, *A&A*, 513, A26
- [21] de León, J., Licandro, J., Serra-Ricart, M., et al. 2010, *A&A*, 517, A23
- [22] DeMeo, F., Binzel, R. P., Slivan, S. M., et al. 2009, *Icarus*, 202, 160
- [23] Duffard, R., Lazzaro, D., Licandro, J., et al. 2004, *Icarus*, 171, 120
- [24] Emery, J. P., Dalle Ore, C. M., Cruikshank, D. P., et al. 2007, *A&A*, 466, 395
- [25] Eugster, O. 2003, *Chem. Erde* 63, 3
- [26] Fornasier, S., Barucci, M. A., Binzel, R. P., et al. 2003, *A&A*, 398, 327
- [27] Gaffey, M. J., & Reddy, V. 2010, in *Lunar and Planetary Institute Science Conference Abstracts*, 41, 1864
- [28] Gaffey, M. J., Burbine, T. H., Piatek, J. L., et al. 1993, *Icarus*, 106, 573
- [29] Guilbert, A., Alvarez-Candal, A., Merlin, F., et al. 2009, *Icarus*, 201, 272

- [30] Hammergren, M., Gyuk, G., & Puckett, A. 2007, *BAAS*, 38, 203
- [31] Hapke, B. 1981, *J. Geophys. Res.*, 86, 3039
- [32] Hapke, B. 1984, *Icarus*, 59, 41
- [33] Hapke, B. 2001, *J. Geophys. Res.*, 106, 10039
- [34] Hutchison, R. 2004, *Meteorites* (Cambridge: Cambridge University Press)
- [35] Jewitt, D. C., & Luu, J. 2007, *Nature*, 432, L731
- [36] Johnson, T. V., & Fanale, F. P. 1973, *J. Geophys. Res.*, 78, 8507
- [37] King, T. V., & Ridley, W. I. 1989, *J. Geophys. Res.*, 92, 11457
- [38] Lazzaro, D., Michtchenko, T., Carvano, J. M., et al. 2000, *Science*, 288, 2033
- [39] Licandro, J., & Pinilla-Alonso, N. 2005, *ApJ*, 630, L93
- [40] Licandro, J., Pinilla-Alonso, N., Pedani, M., et al. 2006a, *A&A*, 445, L35
- [41] Licandro, J., Grundy, W. M., Pinilla-Alonso, N., et al. 2006b, *A&A*, 485, L5
- [42] Licandro, J., Campins, H., Kelley, M., et al. 2011, *A&A*, 525, A34
- [43] Luu, J. X., & Jewitt, D. C. 1998, *ApJ*, 494, L117
- [44] Pieters, C. M., Ficher, E. M., Rode, O. D., et al. 1993, *J. Geophys. Res.*, 98, 20817
- [45] Pinilla-Alonso, N., Licandro, J., Gil-Hutton, R., et al. 2007, *A&A*, 468, L25
- [46] Pompilio, L., Pedrazzi, G., Sgavetti, M., et al. 2009, *Icarus*, 201, 781
- [47] Sagan, C., & Khare, B. N. 1979, *Nature*, 277, 102
- [48] Shaller, E. L., & Brown, M. E. 2007, *ApJ*, 659, L61
- [49] Shkuratov, Y., Starukhina, L., Hoffmann, H., et al. 1999, *Icarus*, 137, 235
- [50] Sunshine, J. M., & Pieters, C. M. 1993, *J. Geophys. Res.*, 98, 9075
- [51] Sunshine, J. M., & Pieters, C. M. 1998, *J. Geophys. Res.*, 103, 13675
- [52] Sunshine, J. M., Pieters, C. M., & Pratt, S. F. 1990, *J. Geophys. Res.*, 95, 6955
- [53] Tholen, D. J. 1984, Ph.D. thesis, AA (Arizona Univ., Tucson)
- [54] Vernazza, P., Binzel, R. P., Thomas, C. A., et al. 2008, *Nature*, 454, L858
- [55] Vilas, F., & Gaffey, M. J. 1989, *Science*, 246, 790
- [56] Wasson, J. T., & Wetherill, G. W. 1979, in *Asteroids*, ed. T. Gehrels (Tucson: University of Arizona Press), 926